Published online 06 May 2014

Nucleic Acids Research, 2014, Vol. 42, No. 11 ***7259–7267***
doi: 10.1093/nar/gku384

Increased negative supercoiling of mtDNA in *TOP1mt* knockout mice and presence of topoisomerases IIα and IIβ in vertebrate mitochondria

Hongliang Zhang[1,*], Yong-Wei Zhang[1], Takehiro Yasukawa[2], Ilaria Dalla Rosa[1], Salim Khiati[1] and Yves Pommier[1,*]

[1]Laboratory of Molecular Pharmacology and Developmental Therapeutics Branch, Center for Cancer Research, National Cancer Institute, National Institutes of Health, Bethesda, MD 20892-4255, USA and [2]The Wolfson Institute for Biomedical Research, University College London, Gower Street, London WC1E 6BT, UK

Received February 26, 2014; Revised April 15, 2014; Accepted April 21, 2014

ABSTRACT

Topoisomerases are critical for replication, DNA packing and repair, as well as for transcription by allowing changes in DNA topology. Cellular DNA is present both in nuclei and mitochondria, and mitochondrial topoisomerase I (Top1mt) is the only DNA topoisomerase specific for mitochondria in vertebrates. Here, we report in detail the generation of *TOP1mt* knockout mice, and demonstrate that mitochondrial DNA (mtDNA) displays increased negative supercoiling in *TOP1mt* knockout cells and murine tissues. This finding suggested imbalanced topoisomerase activity in the absence of Top1mt and the activity of other topoisomerases in mitochondria. Accordingly, we found that both Top2α and Top2β are present and active in mouse and human mitochondria. The presence of Top2α-DNA complexes in the mtDNA D-loop region, at the sites where both ends of 7S DNA are positioned, suggests a structural role for Top2 in addition to its classical topoisomerase activities.

INTRODUCTION

Topoisomerases are ubiquitous enzymes that control the topology of nucleic acids by introducing transient breaks in their phosphodiester backbones (1–4). They are classified as type I and type II topoisomerases, depending whether they act by catalyzing transient single- or double-strand breaks, respectively. Vertebrates have six topoisomerases: Top1 and Top1mt are type IB topoisomerases, Top2α and Top2β are type IIA topoisomerases, and Top3α and Top3β are type IA topoisomerases (2,3); all of which are encoded in the nuclear genome. Top1 and Top1mt (type IB enzymes) act as DNA untwisting enzymes (1,5). They effectively relax both negatively and positively supercoiled DNA (6,7) in the absence of metal or nucleotide cofactor by nicking-closing one strand of duplex DNA while forming 3′-linked tyrosyl-DNA cleavage complexes [see schemes in (3)]. All other metazoan topoisomerases act by forming 5′-linked tyrosyl-DNA cleavage complexes. Top2α and Top2β are the metazoan type IIA enzymes. Their activities require Mg^{2+} and ATP, as they cleave both strands of a DNA duplex in concert, allowing the relaxation of both negative and positive supercoils by strand passage (8–10). Their strand passage mechanism also allows the decatenation of interlocked DNA molecules, an essential function at the end of replication, especially for circular genomes such as mtDNA. Top3α and Top3β are type IA enzymes; they reversibly cleave one strand, changing nucleic acid topology by strand passage of a segment of single-stranded nucleic acid in the presence of magnesium ions but without nucleotide cofactor, which explain why Top3 enzymes relax negatively supercoiled (melted) but not positively supercoiled DNA (1,11) [see schemes in (3)].

Mitochondria are essential for the production of cellular energy in the form of ATP, for synthesizing key cellular metabolites, and for regulating cell survival and death. Unlike other eukaryotic cellular organelles, they contain their own DNA (mtDNA) organized in nucleoids. Each nucleoid contains several identical mtDNA molecules, each consisting of a duplex DNA circle. Because of its circular structure, obligatory transcription and replication, and attachment to the mitochondrial inner membrane, mtDNA

*To whom correspondence should be addressed. Tel: +1 301 496 5944; Fax: 301-402-0752; Email: pommier@nih.gov
Correspondence may also be addressed to Hongliang Zhang. Tel: +1 301 451 8598; Email: hongliangzhang@mail.nih.gov
Present address:
Takehiro Yasukawa, Department of Clinical Chemistry and Laboratory of Medicine, Graduate School of Medical Sciences, Kyushu University, Fukuoka, Japan.

is likely to be highly dependent on topoisomerases. This is especially true because mtDNA is transcribed bidirectionally from three promoters localized in and at the vicinity of the regulatory non-coding region (NCR), which is source of torsional stress (12). Replication of mtDNA also initiates in the NCR, from the light strand promoter, often pausing toward the end of the regulatory region with nascent DNA (7S DNA) displacing the parental strand and generating a D-loop structure (13,14). The mechanism of D-loop formation and the functional roles of 7S DNA remain elusive; the D-loop has been proposed to regulate mtDNA replication (15), scaffold mtDNA and organize nucleoids by mediating their attachment to the mitochondrial inner membrane (16,17).

Until the present report, three DNA topoisomerases had been described in vertebrate mitochondria: one type IB: Top1mt (5); one type IA: Top3α (11,18); and one type IIA: a truncated form of Top2β (19). Both Top3α and truncated Top2β have a dual distribution in mitochondria and the nucleus with the majority located in nuclei. On the other hand, Top1mt is the only DNA topoisomerase specific for mitochondria in vertebrates (5,20). Yet Top1mt is not essential, although its deletion affects mitochondrial integrity and cellular energy metabolism (21). Here, we report in detail the generation of *TOP1mt* knockout mice and *TOP1mt* knockout fibroblasts whose metabolic and autophagic phenotypes were described recently (21). We show that, although viable, *TOP1mt* knockout murine cells harbor increased negative supercoiling of mtDNA. This novel finding prompted us to re-examine the presence of type II topoisomerases (19) in vertebrate mitochondria, and to demonstrate that both full-length Top2α and Top2β are present in mouse and human mitochondria.

MATERIALS AND METHODS

Generation of *TOP1mt* knockout mice

The bacterial artificial chromosome (BAC) clone containing mouse *TOP1mt* genomic DNA was purchased from Incyte Genomics, Inc. Sau3AI partially digested *TOP1mt* genomic DNA was subcloned into pZERO-2 plasmid. A 6.1 kb Sau3AI–HindIII fragment with LoxP and SpeI sites was inserted in front of neomycin resistance gene, and a 3.8 kb HindIII fragment between neomycin resistance gene and thymidine kinase gene. The final construct was linearized with NotI and transfected into TC-1 129SvEv mouse embryonic stem (ES) cells by electroporation. Transfected ES cells were cultured in selection medium with G418 (Geneticin) and FIAU [1-(2-deoxy-2-fluoro-beta-D-arabino furanosyl]-5-iodouracil) and clones were isolated for Southern blot analysis. A 1.4 kb fragment spanning exons 11 and 12 was used as probe. The targeted ES clones were microinjected into C57/BL6 morulas to generate chimeric founder mice. Male chimeric mice were kept for breeding with female C57BL/6 mice to test germline transmission of the targeted *TOP1mt* locus. Next, the male chimeric mice with proven germline transmission ability were bred with the Cre mice.

The locations of PCR primers used for genotyping wild-type (WT) and manipulated *TOP1mt* alleles are indicated in Figure 1A. The primers are *TOP1mt*-A (5′-GGTGCTAGACATTGAACTCAG), *TOP1mt*-B (5′-CTGCAAATGGCCTCGTTAGC), and *TOP1mt*-C (5′-GTCCTGGATTCCATCTTAAGC). Mouse genomic DNA samples were prepared from tail tips following standard protocols. PCR reactions were performed using genomic DNA as templates and *TOP1mt* genotype-specific primer pairs with the following program: 94°C for 2 min; 94°C for 20 s, 55°C for 30 s, 72°C for 20 s for 30 cycles ending with incubation at 72°C for 5 min.

Measurement of mtDNA supercoiling

Total DNA from mouse embryonic fibroblast (MEF) (21) and mice tissues was isolated following standard protocols. For each sample, 2 μg total DNA was separated in 0.3% agarose gel at 4°C overnight and blotted by capillary transfer onto Hybond-N+ membranes (GE Healthcare). The mtDNA was visualized by Southern blotting using the ^{32}P-labeled probe specific for mouse-mtDNA (nucleotide positions 15 007–15 805).

Mapping Top2 sites in mtDNA

A modified version of our PL-PCR (phosphate-linked ligation-mediated PCR) method was used (22). Briefly, DNA samples were directly ligated with annealed phosphate linker with T4 DNA ligase at 16°C overnight. After ligation, samples were PCR-amplified with mtDNA specific primers and a general primer complementary to the linker sequence. A ^{32}P labeled nested (to the specific primer) primer was used to label the PCR products. The labeled PCR products were separated by 6% denaturing polyacrylamide gels, and visualized by PhosphoImager®. Bands of interest were sequenced to determine the genomic positions of the cleavage sites (22).

Preparation of mitochondria

Mitochondrial were prepared as described (22). Briefly, cell pellets were suspended in CaRSB buffer (10 mM of NaCl, 1.5 mM $CaCl_2$ and 10 mM Tris–HCl, pH 7.5 at 25°C) for 5 min. Following osmotic shock, cells were homogenized using a glass Dounce homogenizer (35 strokes). One-sixth volume of stabilizing buffer (2 M sucrose, 35 mM EDTA, and 50 mM Tris–HCl, pH 7.5 at 25°C) was added to cell lysates, and mixed with two additional strokes with glass Dounce homogenizer. Cell lysates were centrifuged at 750 *g* for 5 min to remove nuclei and cell debris. Supernatants were collected and the previous step was repeated one more time. The mitochondria were spun down from supernatant at 10 000 *g* for 20 min and washed with MT buffer (250 mM sucrose, 10 mM KCl, 1.5 mM $MgCl_2$, 1 mM EDTA (Ethylenediaminetetraacetic acid), 1 mM EGTA (ethylene glycol tetraacetic acid), 5 mM DTT (Dithiothreitol) and 20 mM HEPES(4-(2-hydroxyethyl)-1-piperazineethanesulfonic acid)–KOH, pH 7.4 at 25°C) and re-suspended in MT buffer.

Western blotting

MCF7 mitochondrial lysates were resolved by SDS-polyacrylamide gel electrophoresis (SDS-PAGE) (6%), and

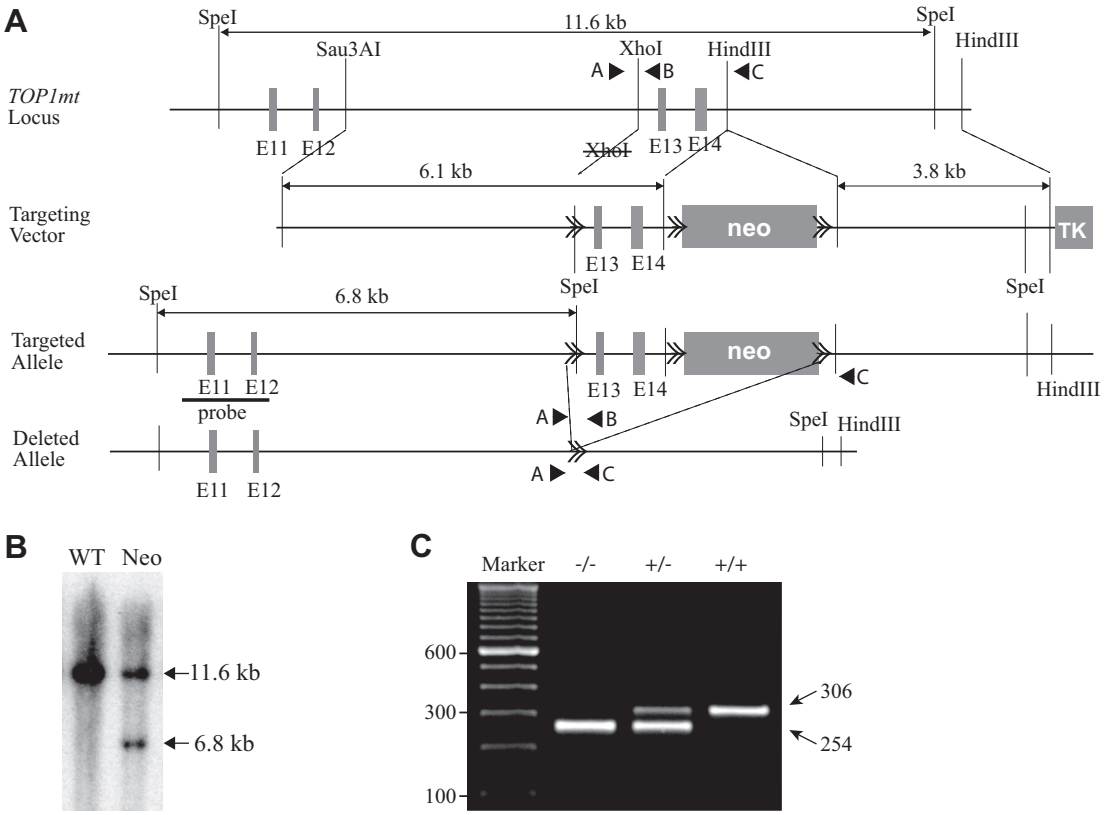

Figure 1. *TOP1mt* knockout strategy. (**A**) Genetic constructs used for knocking out *TOP1mt*. Restriction enzyme sites are marked as vertical lines. Exons are labeled E11, E12, E13 and E14, among which the last two exons were targeted for knockout. Exon 13 contains the catalytic tyrosine of Top1mt. Positive selection neomycin (neo) gene and negative selection thymidine kinase (TK) gene are indicated. LoxP sites are marked as double arrowheads. PCR primers (A, B and C) are marked as black triangles. (**B**) Southern blotting showing the targeted *TOP1mt* allele. SpeI digestion generates a 6.8 kb band in the targeted allele (11.6 kb in wild-type). (**C**) PCR genotyping. Wild-type *TOP1mt* gives a 306 bp band, and the deletion form*s* a 254 bp. Heterozygous mice show both bands.

transferred onto nitrocellulose membranes (Bio-Rad, Hercules, CA, USA). After blocking non-specific binding for 1 h with 5% milk in TPBS (phosphate-buffered saline, Tween20 0.1%), membranes were incubated overnight with primary antibody: C-21 for Top1 (#556597, BD Pharmingen), Ki-S1 for human Top2α (Millipore, Bedford, MA, USA), sc-365916 for mouse Top2α (Santa Cruz Biotechnology, Santa Cruz, CA, USA), and sc-25330 for Top2β (Santa Cruz Biotechnology, Santa Cruz, CA, USA). After three washes in TPBS, the membrane was incubated with horseradish peroxidase-conjugated goat anti-mouse antibody (Amersham Biosciences, Piscataway, NJ, USA) for 1 h and then washed three times in TPBS. Immunoblots were revealed using enhanced chemiluminescence detection kit (Pierce).

Immunoprecipitation and mass spectrometry

Purified mitochondria were lysed in 10 mM Tris–HCl, pH 8.0, 450 mM NaCl, 1% Triton X-100, 0.1% SDS, 1 mM DTT, 1 mM EDTA, with protease inhibitor cocktail. Cleared mitochondrial extract was incubated with antibody PA1-21150 (ABR), generated against full-length human Top2β for 4 h. Protein A/G agarose was added, and incubated for overnight. After three washes, immunoprecipitated proteins were resolved on 6% Tris–glycine gel. The prominent protein bands were excised and analyzed by mass spectrometry (MS).

ICE bioassay

In vivo complex of enzyme (ICE) bioassays were performed as described (22,23). Mitochondrial lysates from MCF7 cells treated with etoposide (VP-16) were lysed with 1% sarkosyl and gently loaded on top of a CsCl gradient. After ultracentrifugation (125 000 *g* for 20 h at 20°C), the samples were collected from the bottom of the centrifuge tubes, and transferred to the Immobilon-P membrane (Millipore, Bedford, MA, USA). Top2 was detected using standard western blotting protocol with antibody PA1-21150 (ABR).

Immunofluorescence assays

Immunofluorescence microscopy was performed as described (24). The anti-Top2β (sc-25330) primary antibody and blocking peptide were from Santa Cruz Biotechnology

(Santa Cruz, CA, USA). The anti-Top2α (Ki-S1) primary antibody was from Millipore (Bedford, MA, USA).

RESULTS

Generation of the *TOP1mt* knockout mice

First, to complement our recent publication (21) and an upcoming one (25), we provide here a full description of the methodology and rationale for generating our *TOP1mt* knockout mice. The human and mouse *TOP1mt* genes consist of 14 conserved exons encoding 601 and 593 amino acid polypeptides, respectively (20). The last 13 exons are highly conserved with the nuclear *TOP1* genes, whereas the first exon encodes a short N-terminal segment with a mitochondrial targeting signal (5,20). The catalytic tyrosine residue of Top1mt is located in exons 13, which was targeted for knocking out the gene (Figure 1A).

Because nuclear *TOP1* knockout mice are early embryonic lethal (26), and because previously studied genes involved in mitochondrial DNA activity, such as the mitochondrial transcription factor A (TFAM) are essential (27), we chose a Cre-mediated conditional system to knockout the *TOP1mt* gene (Figure 1). The XhoI restriction enzyme site in front of exon 13 was converted to a LoxP and SpeI site for selection (Figure 1A). The targeting vector contained a 6.1 kb 5′-targeting arm with the LoxP and Spe1 sites, a neo expression cassette for positive selection, a 3.8-kb 3′-targeting arm, and a thymidine kinase (TK) expression cassette for negative selection (Figure 1A). Because of two LoxP sites flanking the neo gene, exons 13 and 14 were flanked by LoxP sites.

After 129SvEv mouse ES cells were transfected with the targeting vector and cultured in selection medium with G418 and FIAU, 192 clones were selected. DNA samples were prepared from those clones for Southern blot screening. The fragment containing exons 11 and 12 was used as probe. This probe detected a 6.8 kb targeted allele band in addition to a 11.6 kb WT allele band from SpeI-digested DNA samples (Figure 1B). Together, 12 positive clones out of 192 isolates (6.25%) were detected. Targeted ES clones were microinjected into C57BL/6 blastocysts to generate chimeric mice. Male chimeras were kept for testing germline transmission of the $TOP1mt^{f\text{-neo}}$ allele by crossing with C57BL/6 female mice and by examining the coat color of their offspring. Agouti coat indicates a germline transmission from the 129SvEv ES cell, while black coat indicates a C57BL/6 blastocyst donor origin. A total of 10 chimeric founder mice were identified. To maximize survival, mice of different background were used for breeding. We crossed $TOP1mt^{+/f}$ mice with EIIa-Cre transgenic mice with a FVB background to generate $TOP1mt^{+/f}$/EIIa-Cre mice with a mixed genetic background. Cre converted $TOP1mt^{+/f}$ to $TOP1mt^{+/-}$, and the produced heterozygous $TOP1mt^{+/-}$ mice were genotyped by PCR with tail-tip DNA samples. $TOP1mt^{+/-}$ mice were crossed to generate $TOP1mt^{+/+}$, $TOP1mt^{+/-}$ and $TOP1mt^{-/-}$ mice (Figure 1C).

Unexpectedly, $TOP1mt^{-/-}$ mice are viable and fertile, and we recently reported that MEF cells derived from such mice display defective oxidative phosphorylation, increased glycolysis and fatty acid oxidation, and an accumulation of reactive oxygen species (21). We also recently showed that $TOP1mt^{-/-}$ mice are hypersensitive to doxorubicin-induced cardiotoxicity (25). Because *TOP1mt* knockout mice are viable and fertile, in the present study we were able to study their mtDNA.

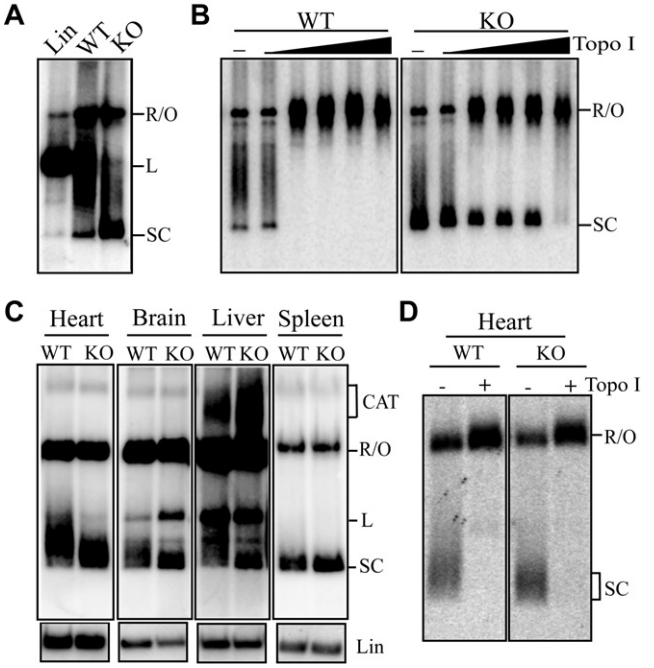

Figure 2. Increased negative supercoiling of mtDNA in *TOP1mt* knockout cells. (**A**) Southern blot analyses of mtDNA isolated from wild-type (WT) and *TOP1mt* knockout (KO) murine embryonic fibroblasts (MEFs). Lin, linearized control mtDNA. Topoisomers are indicated at right: SC, supercoiled; L, linear; R/O, relaxed/open. (**B**) Negative supercoiling of mtDNA. mtDNA from WT and KO MEFs was incubated with increasing concentrations of *Escherichia coli* topoisomerase I (Topo I). (**C**) Analysis of the indicated murine tissues showing increased negative supercoiling of their mtDNA. (**D**) Relaxation of heart mtDNA by *E. coli* topoisomerase I.

Increased negative supercoiling of mtDNA in the $TOP1mt^{-/-}$ cells and tissues

First, we analyzed mtDNA from $TOP1mt^{-/-}$ MEF cells (21). Southern blot analyses showed a significant increase in supercoiled (SC) mtDNA molecules in $TOP1mt^{-/-}$ MEF cells (Figure 2A). To determine whether such supercoils were positive (overwinding) or negative (underwinding) (4), we incubated mtDNA with *Escherichia coli* topoisomerase I, a type IA topoisomerase (1–3), which only relaxes negatively supercoiled DNA. *E. coli* topoisomerase I fully relaxed the supercoils, indicating that the mtDNA of $TOP1mt^{-/-}$ cells is negatively supercoiled, as it is the case for most natural purified DNA. We also noticed that more *E. coli* topoisomerase I was required to fully relax the mtDNA of $TOP1mt^{-/-}$ than that of WT $TOP1mt^{+/+}$ MEF cells. Combined with the Southern blot results showing increased supercoiled mtDNA in $TOP1mt^{-/-}$ MEF cells, the *E. coli* topoisomerase I relaxation results indicate that mtDNA of *TOP1mt* knockout MEF cells exhibits increased negative supercoiling (Figure 2A).

Next, we analyzed mouse tissues from the *TOP1mt* knockout animals. Compared with their WT counterpart,

TOP1mt knockout mice showed increased mtDNA supercoiling in all tested tissues: heart, brain, liver and spleen (Figure 2B). These results are consistent with those obtained in *TOP1mt*$^{-/-}$ MEF cells, and demonstrate a specific role for Top1mt in relaxing mtDNA negative supercoiling. Moreover, the increased negative supercoiling in *TOP1mt*$^{-/-}$ MEF cells and murine tissues implies the existence of a mitochondrial topoisomerase activity that efficiently relaxes positive mtDNA supercoiling.

Top2α and Top2β are present in human and mouse mitochondria

Given that topoisomerases are essential, we posited that the viability of *TOP1mt* knockout mice must come from compensation by other topoisomerase(s). We eliminated complementation by nuclear Top1, as repeated attempts showed that the enzyme was undetectable in mitochondria (Figure 3A, bottom panel for a representative experiment). Moreover, introduction of Top1 in mitochondria depletes mtDNA and is toxic to mitochondria (28). Although a mitochondrial isoform of Top3α is present in mitochondria (11,18), Top3α is also unlikely to compensate for lack of Top1mt because type IA topoisomerases (Top3α and Top3β) preferentially process single-stranded DNA segments (hypernegatively supercoiled) and therefore drive DNA supercoiling toward positive (29,30) (see 'Introduction' section), which is opposite to the results of *TOP1mt* knockout mtDNA. On the other hand, Top2α and Top2β can remove positive supercoils with high efficiency (31), and a truncated form of Top2β has been reported in bovine heart mitochondria (19).

Hence, we tested the presence of Top2β in mitochondria. Western blotting of human breast cancer MCF-7 cells showed a clear signal (Figure 3A). However, unlike previously reported (19), Top2β appeared full-length (Figure 3A). Lamin B1 (LMNB1) and TFAM were used as nuclear (N) and mitochondrial (M) controls, respectively. As indicated above, nuclear Top1 was present only in the nuclear fractions, and therefore served as an additional nuclear marker and quality control. When the same membranes were stripped and re-blotted with antibodies specific for Top2α and Top2β (Figure 3A, top panels), not only Top2β but also Top2α gave full-length signal, indicating that both Top2α and Top2β exist at relatively high levels and as full-length polypeptides in human mitochondria.

To confirm and extend our discovery that both Top2α and Top2β are present in vertebrate mitochondria, we performed immunofluorescence microscopy with murine tissues and human cells. In mouse retina, Top2α and Top2β were clearly detectable in the mitochondrial layer, as mitochondria form a well-defined layer in the inner segment (IS), apart from nuclei (32) (Figure 3B and C). Next, we extended the immunofluorescence studies to human osteosarcoma U2OS cells, which give clear mitochondrial signals. Figure 3D shows the presence of Top2α both in the nuclei and mitochondria of U2OS cells. In vertebrate sperms, mitochondria are concentrated in the mid-piece separated from the head containing the condensed nucleus (Figure 3D). Top2β was readily detected in the mitochondria (Figure 3E) (33). A cognate blocking peptide diminished the Top2β signal, thereby demonstrating its specificity (Figure 3F). On the other hand, Top2α was undetectable in sperm mitochondria, which is consistent with the lack of Top2α expression in most non-proliferating cells and tissues (34).

To gain further evidence for the presence of full-length Top2α and Top2β in mitochondria, we performed immunoprecipitation experiments with purified mitochondrial lysates. Samples resolved by SDS-PAGE showed two prominent protein bands, at approximately 180 and 150 kDa (Figure 4, left inset). Analysis of both bands by MS showed multiple peptides matching sequences that are common to both Top2α and Top2β (Figure 4, yellow). Moreover, Top2β specific peptides mapped throughout the protein sequence (Figure 4, green), confirming that full-length Top2β localizes to mitochondria. Top2α specific peptides were also revealed by the MS analyses (Figure 4, red).

Together, the western blotting, immunofluorescence and MS results demonstrate the presence of both full-length Top2α and Top2β in mammalian mitochondria.

Top2α activity in mitochondria

To detect Top2 activity in mitochondria, we took advantage of the fact that type II topoisomerases cleave the DNA backbone by covalent attachment to the 5′-ends of the break, and that these transient catalytic intermediates, which are referred to as cleavage complexes (2,3) can be trapped by etoposide, a selective Top2α–Top2β poison widely used for cancer treatment (3,35,36). Consistent with the presence of Top2α and Top2β in mitochondria, treatment of purified mitochondria from MCF-7 cells with etoposide generated Top2-DNA complexes, as measured by the ICE bioassay (22,23) (Figure 5A).

Next, we focused on the mapping of Top2α sites in mtDNA. To do so, we first produced *TOP1mt-TOP2B* double-knockout mice. Consistent with the prior report for single *TOP2B* knockout mice (37), the *TOP1mt-TOP2B* double-knockout mice died at birth. Nevertheless, we were able to establish *TOP1mt-TOP2B* double-knockout MEF. Using these cells and PL-PCR (22), we detected etoposide-induced DNA breaks, and were able to map Top2α cleavage sites in mtDNA. A typical example is shown in Figure 5B and C for the NCR of mtDNA. Etoposide-induced bands were sequenced and corresponding cleavage sites were marked with their genomic positions (Figure 5B and C). These experiments demonstrate that Top2α is functionally active in mitochondria.

Top2α-mtDNA complexes at the ends of 7S DNA

During the process of mapping Top2α cleavage sites, the L16038 site in the mtDNA non-coding regulatory region (NCR) appeared particularly interesting. It was surprising that this cleavage site existed in MEF mtDNA under normal growth conditions in the absence of Top2 inhibitor. Compared with the drug-induced sites, the L16038 site was consistently more intense; for instance, in the representative experiment shown in Figure 5D, the L16038 cleavage site was more intense than the "Ref" site, which itself was more intense than the drug-induced sites in Figure 5B. The L16038 site was mapped to the L-strand at a position opposite to the bond between the first and second nucleotides of

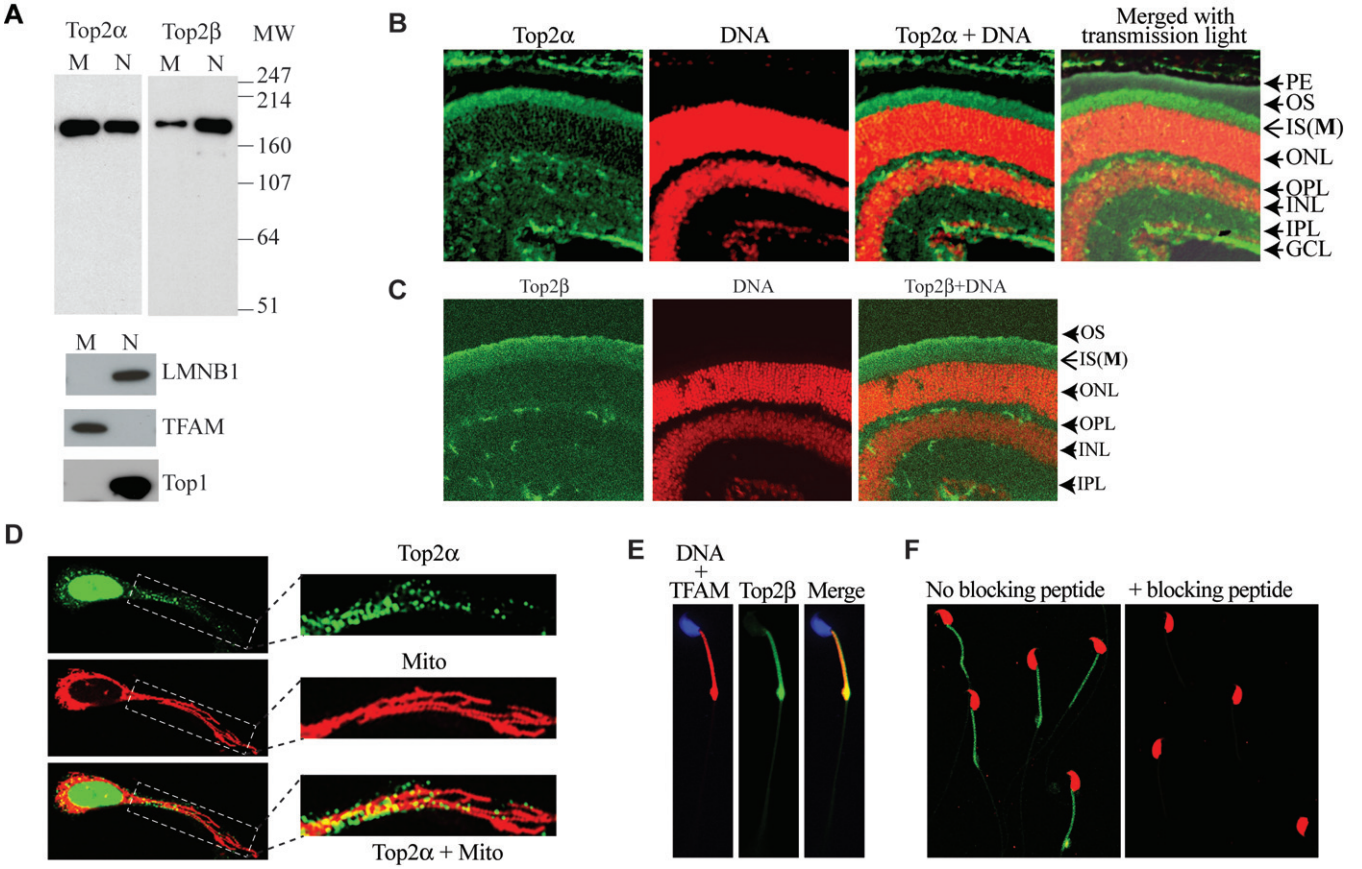

Figure 3. Top2α and Top2β are present in human and murine mitochondria. (**A**) Western blots of mitochondrial (M) and nuclear (N) extracts for Top2α and Top2β in MCF7 cells. LamB1 and Top1 were used as nuclear proteins, and TFAM as mitochondrial protein control. (**B**) Representative immunofluorescence microscopy image of Top2α in mouse retina. Top2α and DNA are green and red, respectively. PE, pigment epithelium; OS, outer segment; IS, inner segment (mitochondria segment); ONL, outer nuclear layer; OPL, outer plexiform layer; INL, inner nuclear layer; IPL, inner plexiform layer; GCL, ganglion cell layer. (**C**) Same as (B) for Top2β. (**D**) Top2α (green) staining in mitochondrial of human osteosarcoma U2OS cells. Cells were transfected with mitochondria-YFP plasmid to label mitochondria (red). Right panels show magnified images of the areas outlined in the left panels. (**E**) Immunofluorescence microscopy images of Top2β in mouse sperm cells. Top2β is in green, TFAM in red and DNA in blue. (**F**) Suppression of the Top2β signal by Top2β blocking peptide.

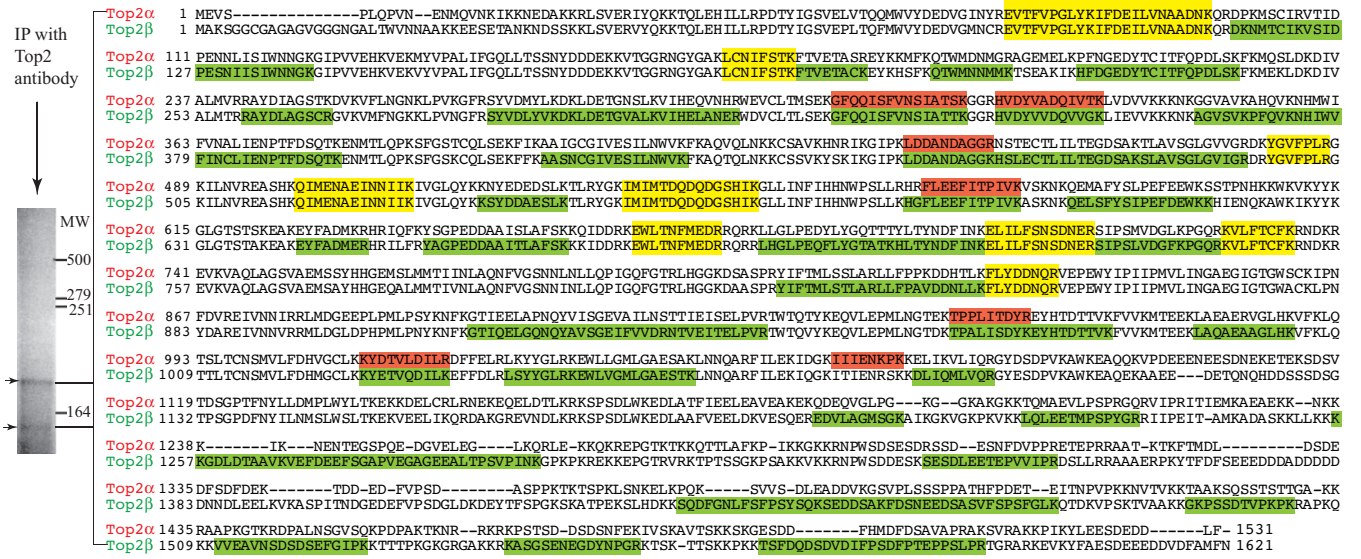

Figure 4. Both Top2α and Top2β can be detected in mitochondria by mass spectrometry (MS). (Left) Proteins from immunoprecipitation used for MS analysis. Two main protein bands, approximately 180 and 150 kDa (arrowheads) were selected for MS analysis. (Right) MS analysis results shown in Top2α and Top2β alignment format. Fragments unique to Top2α are in red, unique to Top2β in green and common to both Top2α and Top2β in yellow.

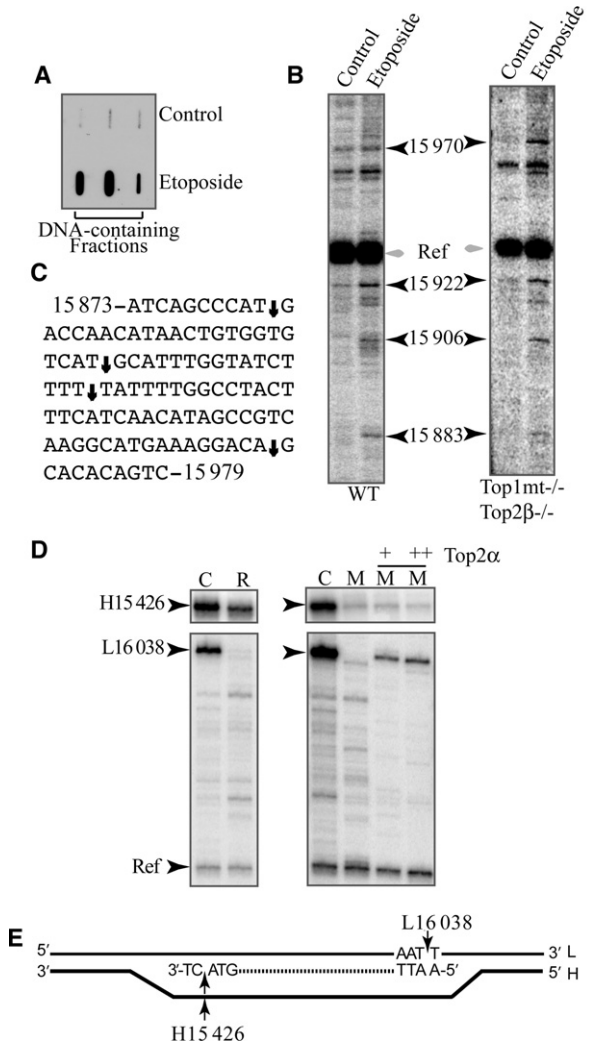

Figure 5. Top2 cleavage complexes in mtDNA. (**A**) Top2 cleavage complexes in mitochondria from MCF7 cells treated with etoposide. Mitochondrial lysates were fractioned by CsCl gradient. Three consecutive DNA-containing fractions of each sample were collected and immunoblotted with Top2 antibody (ICE bioassay). (**B**) Cleavage sites in mtDNA from *TOP1mt TOP2β* double-knockout MEFs and their wild-type (WT) counterpart treated with etoposide. PL-PCR was used to visualize mtDNA fragments. Ref: non-specific band used as reference. (**C**) Map summarizing the etoposide-induced cleavage sites shown in panel (B) (arrows). (**D**) Characterization of the Top2α site at nucleotide positions H15 426 and L16 038 observed under normal growth conditions. Both sites were characterized with respect to heat-reversibility (R) (65°C for 5 min), merbarone-sensitivity (M) (200 μM for 4 h) and regeneration by addition of purified human Top2α to mtDNA from merbarone-treated cells. (**E**) Schematic drawing showing the notable position of the H15 426 and L16 038 sites. The 7S DNA in the D-loop is shown as dashed line.

the 7S DNA 5′-end (38) (Figure 5D and E). This cleavage site was reversible by brief heating of 65°C for 5 min (39) and was suppressed by merbarone (Figure 5D), a known catalytic Top2 inhibitor (35,40). These characteristics meet the criteria of Top2-mediated DNA breaks. Although Top2 tends to generate concerted double-strand DNA breaks, we did not detect the corresponding break on the other strand (H-strand), suggesting that the L16038 break happens only when mtDNA is in D-loop configuration (Figure 5E). We recapitulated the break with purified human Top2α and mtDNA from merbarone-treated MEF cells (Figure 5D), which provided further evidence that the L16038 cleavage site was mediated by Top2α.

At the 3′-end of the 7S DNA region, another Top2α cleavage complex was found at position H15426 (Figure 5D), two nucleotides away from the 3′-end (41). Similar to the L16308 site, the H15426 site was intense in the absence of etoposide treatment and merbarone sensitive. Unlike the L16308 site, the H15426 site could not be recapitulated by incubating the mtDNA obtained from merbarone-treated cells with purified human Top2α. We also noticed that the H15426 site could be only partially reversed by brief heating of 65°C for 5 min.

DISCUSSION

To study Top1mt functions, we generated *TOP1mt* knockout mice using the strategy described in Figure 1. The viability of *TOP1mt* knockout mice, which we first reported in a study focusing on their mitochondrial dysfunctions (21) was unexpected because: (i) knocking out nuclear Top1 is embryonic lethal (26,42), as is knocking out other nuclear encoded mtDNA homeostasis genes, (ii) because Top1mt is present and conserved in all vertebrates (20,43) and (iii) because Top1mt is the only mitochondrial-specific topoisomerase. In spite of the viability and fertility of *TOP1mt* knockout mice, we recently showed that *TOP1mt* knockout mice are hypersensitive to doxorubicin and die from doxorubicin-induced cardiac failure with extensive mitochondrial damage (25), probably because the mtDNA damage produced by doxorubicin-induced Top2β cleavage complexes (44) cannot be efficiently compensated by mtDNA regeneration in *TOP1mt* knockout mice (25). In the present study, we show that mtDNA from the *TOP1mt* knockout cells and murine tissues exhibits increased supercoiling, which is consistent with the efficient DNA untwisting activity of Top1mt (5,6). As this supercoiling could be resolved by *E. coli* topoisomerase I, which only relaxes negatively supercoiled DNA, we conclude that lack of Top1mt leads to an increased negative supercoiling of mtDNA. This finding implies that unwinding negative supercoiling is a prominent function of Top1mt, and that other mitochondrial topoisomerases are insufficient to fully complement for lack of Top1mt. The difference in outcome between the early embryonic lethality of (nuclear) *TOP1* knockout mice (26,42) and the survival of *TOP1mt* knockout mice probably reflects the more complex regulatory functions of (nuclear) Top1 (45), and the differential topological requirements between the mitochondrial and nuclear genomes. The relatively simple mtDNA structure might tolerate topological stress such as the increase in negative supercoiling observed in *TOP1mt* knockout cells, whereas the nuclear genome becomes unstable and accumulates endogenous DNA breaks upon *TOP1* knockdown (45).

Given that topoisomerase activity is required for normal DNA functions (1,2), the viability of *TOP1mt* knockout mice demonstrates compensation by other topoisomerases. Although we cannot rule out the possibility that a small fraction of nuclear Top1 has access to the mitochondria, all our biochemical and biological data argue against the

presence of nuclear Top1 in mitochondria. Moreover, the increased negative supercoiling of mtDNA in the absence of Top1mt implies that mitochondria contain an efficient topoisomerase activity that relaxes DNA positive supercoiling (46,47). Our study shows that Top2α and Top2β can act in such fashion, as they are present and active in human and murine mitochondria. Both Top2α and Top2β were readily detectable in human breast cancer MCF7 cells not only in the nuclear compartment but also in mitochondria, and we estimate that the content of Top2α and Top2β is approximately two orders of magnitude lower in mitochondria than in the nucleus of exponentially growing cells. The relative contribution of Top2α and Top2β to mitochondria is likely to be dependent on cell growth conditions (34) and to be tissue specific. Unlike Top2α, Top2β was readily detectable in sperm mitochondria. Also, Top2α is expressed at very low levels in heart (48), and it is likely that in such tissues, Top2β is the prevalent type II topoisomerase both in the nuclear and mitochondrial compartments. This probably explains why a prior study detected only Top2β in bovine heart (19). On the other hand, Top2α tends to be highly expressed in cancer tissues.

Our study establishes that both type IIA topoisomerases Top2α and Top2β act as mitochondrial enzymes in addition to their critical nuclear functions in vertebrates. Immunoblotting and MS analyses demonstrate that the mitochondrial forms of Top2α and Top2β are full-length polypeptides, which questions the previous conclusion that C-terminal truncation was a characteristics of mitochondrial Top2β (19). In keeping with the fact that many other proteins acting in mitochondria do not contain recognizable mitochondrial targeting sequences, we could not identify mitochondrial targeting sequences in Top2α and Top2β, suggesting they are likely transported into mitochondria with cryptic mitochondrial targeting signals and/or other mitochondrial carriers (49).

Type IIA topoisomerases in mitochondria are likely to be critical not only for relaxing supercoiling associated with transcription and replication, but also, and most critically for decatenating mtDNA circles during and following their replication. Although our study does not address whether Top2α and Top2β exhibit distinct mitochondrial functions in cells expressing both enzymes, the presence of preferential Top2α cleavage complexes at the ends of the D-loop region is noteworthy. Such sites might be related to non-canonical functions of Top2 in mtDNA. Some special DNA structures tend to form relatively stable Top2-DNA complexes (50), and in the case of the mtDNA D-loop region, the observed Top2 sites might be involved in scaffolding the NCR and protecting the 7S DNA ends from degradation, as has been proposed for telomeres (51,52).

ACKNOWLEDGMENTS

We thank Dr Leroy F. Liu for supplying the *TOP2B* mice and Dr Neil Osheroff for Top2α enzyme. We thank Dr Hong Liu and Dr Pedro Echave for technical assistance.

FUNDING

NIH Intramural Program, Center for Cancer Research, National Cancer Institute [Z01 BC 006161]; Biotechnology and Biological Sciences Research Council (UK) David Phillips Fellowship (to T.Y.). Funding for open access charge: NIH Intramural Program, Center for Cancer Research, National Cancer Institute [Z01 BC 006161].
Conflict of interest statement. None declared.

REFERENCES

1. Champoux,J.J. (2001) DNA topoisomerases: structure, function, and mechanism. *Annu. Rev. Biochem.*, **70**, 369–413.
2. Wang,J.C. (2002) Cellular roles of DNA topoisomerases: a molecular perspective. *Nat. Rev. Mol. Cell Biol.*, **3**, 430–440.
3. Pommier,Y., Leo,E., Zhang,H. and Marchand,C. (2010) DNA topoisomerases and their poisoning by anticancer and antibacterial drugs. *Chem. Biol.*, **17**, 421–433.
4. Schoeffler,A.J. and Berger,J.M. (2008) DNA topoisomerases: harnessing and constraining energy to govern chromosome topology. *Q. Rev. Biophys.*, **41**, 41–101.
5. Zhang,H., Barcelo,J.M., Lee,B., Kohlhagen,G., Zimonjic,D.B., Popescu,N.C. and Pommier,Y. (2001) Human mitochondrial topoisomerase I. *Proc. Natl. Acad. Sci. U.S.A.*, **98**, 10608–10613.
6. Seol,Y., Zhang,H., Pommier,Y. and Neuman,K.C. (2012) A kinetic clutch governs religation by type IB topoisomerases and determines camptothecin sensitivity. *Proc. Natl. Acad. Sci. U.S.A.*, **109**, 16125–16130.
7. Koster,D.A., Croquette,V., Dekker,C., Shuman,S. and Dekker,N.H. (2005) Friction and torque govern the relaxation of DNA supercoils by eukaryotic topoisomerase IB. *Nature*, **434**, 671–674.
8. Nitiss,J.L. (2009) DNA topoisomerase II and its growing repertoire of biological functions. *Nat. Rev. Cancer*, **9**, 327–337.
9. Seol,Y., Gentry,A.C., Osheroff,N. and Neuman,K.C. (2013) Chiral discrimination and Writhe-dependent relaxation mechanism of human topoisomerase IIalpha. *J. Biol. Chem.*, **288**, 13695–13703.
10. McClendon,A.K. and Osheroff,N. (2006) The geometry of DNA supercoils modulates topoisomerase-mediated DNA cleavage and enzyme response to anticancer drugs. *Biochemistry*, **45**, 3040–3050.
11. Wu,J., Feng,L. and Hsieh,T.S. (2010) Drosophila topo IIIalpha is required for the maintenance of mitochondrial genome and male germ-line stem cells. *Proc. Natl. Acad. Sci. U.S.A.*, **107**, 6228–6233.
12. Liu,L.F. and Wang,J.C. (1987) Supercoiling of the DNA template during transcription. *Proc. Natl. Acad. Sci. U.S.A.*, **84**, 7024–7027.
13. Shadel,G.S. and Clayton,D.A. (1997) Mitochondrial DNA maintenance in vertebrates. *Annu. Rev. Biochem.*, **66**, 409–435.
14. Kasamatsu,H., Robberson,D.L. and Vinograd,J. (1971) A novel closed-circular mitochondrial DNA with properties of a replicating intermediate. *Proc. Natl. Acad. Sci. U.S.A.*, **68**, 2252–2257.
15. Holt,I.J. and Reyes,A. (2012) Human mitochondrial DNA replication. *Cold Spring Harb. Perspect. Biol.*, **4**.
16. Holt,I.J., He,J., Mao,C.C., Boyd-Kirkup,J.D., Martinsson,P., Sembongi,H., Reyes,A. and Spelbrink,J.N. (2007) Mammalian mitochondrial nucleoids: organizing an independently minded genome. *Mitochondrion*, **7**, 311–321.
17. Bogenhagen,D.F., Rousseau,D. and Burke,S. (2008) The layered structure of human mitochondrial DNA nucleoids. *J. Biol. Chem.*, **283**, 3665–3675.
18. Wang,Y., Lyu,Y.L. and Wang,J.C. (2002) Dual localization of human DNA topoisomerase IIIalpha to mitochondria and nucleus. *Proc. Natl. Acad. Sci. U.S.A.*, **99**, 12114–12119.
19. Low,R.L., Orton,S. and Friedman,D.B. (2003) A truncated form of DNA topoisomerase IIbeta associates with the mtDNA genome in mammalian mitochondria. *Eur. J. Biochem.*, **270**, 4173–4186.
20. Zhang,H., Meng,L.H., Zimonjic,D.B., Popescu,N.C. and Pommier,Y. (2004) Thirteen-exon-motif signature for vertebrate nuclear and mitochondrial type IB topoisomerases. *Nucleic Acids Res.*, **32**, 2087–2092.
21. Douarre,C., Sourbier,C., Dalla Rosa,I., Brata Das,B., Redon,C.E., Zhang,H., Neckers,L. and Pommier,Y. (2012) Mitochondrial topoisomerase I is critical for mitochondrial integrity and cellular energy metabolism. *PLoS One*, **7**, e41094.
22. Zhang,H. and Pommier,Y. (2008) Mitochondrial topoisomerase I sites in the regulatory D-loop region of mitochondrial DNA. *Biochemistry*, **47**, 11196–11203.

23. Subramanian,D., Kraut,E., Staubus,A., Young,D.C. and Muller,M.T. (1995) Analysis of topoisomerase I/DNA complexes in patients administered topotecan. *Cancer Res.*, **55**, 2097–2103.
24. Zhang,Y.W., Jones,T.L., Martin,S.E., Caplen,N.J. and Pommier,Y. (2009) Implication of checkpoint kinase-dependent up-regulation of ribonucleotide reductase R2 in DNA damage response. *J. Biol. Chem.*, **284**, 18085–18095.
25. Khiati,S., Dalla Rosa,I., Sourbier,C., Ma Xufei,, Rao,V.A., Neckers,L., Zhang,H. and Pommier,Y. (2014) Mitochondrial topoisomerase I (Top1mt) is a novel limiting factor of doxorubicin cardiotoxicity. *Clin. Cancer Res.*, in press.
26. Morham,S.G., Kluckman,K.D., Voulomanos,N. and Smithies,O. (1996) Targeted disruption of the mouse topoisomerase I gene by camptothecin selection. *Mol. Cell. Biol.*, **16**, 6804–6809.
27. Larsson,N.G., Wang,J., Wilhelmsson,H., Oldfors,A., Rustin,P., Lewandoski,M., Barsh,G.S. and Clayton,D.A. (1998) Mitochondrial transcription factor A is necessary for mtDNA maintenance and embryogenesis in mice. *Nat. Genet.*, **18**, 231–236.
28. Dalla Rosa,I., Goffart,S., Wurm,M., Wiek,C., Essmann,F., Sobek,S., Schroeder,P., Zhang,H., Krutmann,J., Hanenberg,H. *et al.* (2009) Adaptation of topoisomerase I paralogs to nuclear and mitochondrial DNA. *Nucleic Acids Res.*, **37**, 6414–6428.
29. Hanai,R., Caron,P.R. and Wang,J.C. (1996) Human TOP3: a single-copy gene encoding DNA topoisomerase III. *Proc. Natl. Acad. Sci. U.S.A.*, **93**, 3653–3657.
30. Ng,S.W., Liu,Y., Hasselblatt,K.T., Mok,S.C. and Berkowitz,R.S. (1999) A new human topoisomerase III that interacts with SGS1 protein. *Nucleic Acids Res.*, **27**, 993–1000.
31. McClendon,A.K., Gentry,A.C., Dickey,J.S., Brinch,M., Bendsen,S., Andersen,A.H. and Osheroff,N. (2008) Bimodal recognition of DNA geometry by human topoisomerase II alpha: preferential relaxation of positively supercoiled DNA requires elements in the C-terminal domain. *Biochemistry*, **47**, 13169–13178.
32. Nickell,S., Park,P.S., Baumeister,W. and Palczewski,K. (2007) Three-dimensional architecture of murine rod outer segments determined by cryoelectron tomography. *J. Cell Biol.*, **177**, 917–925.
33. Meyer-Ficca,M.L., Lonchar,J.D., Ihara,M., Meistrich,M.L., Austin,C.A. and Meyer,R.G. (2011) Poly(ADP-ribose) polymerases PARP1 and PARP2 modulate topoisomerase II beta (TOP2B) function during chromatin condensation in mouse spermiogenesis. *Biol. Reprod.*, **84**, 900–909.
34. Heck,M.M. and Earnshaw,W.C. (1986) Topoisomerase II: a specific marker for cell proliferation. *J. Cell Biol.*, **103**, 2569–2581.
35. Nitiss,J.L. (2009) Targeting DNA topoisomerase II in cancer chemotherapy. *Nat. Rev. Cancer*, **9**, 338–350.
36. McClendon,A.K. and Osheroff,N. (2007) DNA topoisomerase II, genotoxicity, and cancer. *Mutat. Res.*, **623**, 83–97.
37. Yang,X., Li,W., Prescott,E.D., Burden,S.J. and Wang,J.C. (2000) DNA topoisomerase IIbeta and neural development. *Science*, **287**, 131–134.
38. Gillum,A.M. and Clayton,D.A. (1979) Mechanism of mitochondrial DNA replication in mouse L-cells: RNA priming during the initiation of heavy-strand synthesis. *J. Mol. Biol.*, **135**, 353–368.
39. Hsiang,Y.H. and Liu,L.F. (1989) Evidence for the reversibility of cellular DNA lesion induced by mammalian topoisomerase II poisons. *J. Biol. Chem.*, **264**, 9713–9715.
40. Fortune,J.M. and Osheroff,N. (1998) Merbarone inhibits the catalytic activity of human topoisomerase IIalpha by blocking DNA cleavage. *J. Biol. Chem.*, **273**, 17643–17650.
41. Doda,J.N., Wright,C.T. and Clayton,D.A. (1981) Elongation of displacement-loop strands in human and mouse mitochondrial DNA is arrested near specific template sequences. *Proc. Natl. Acad. Sci. U.S.A.*, **78**, 6116–6120.
42. Lee,M.P., Brown,S.D., Chen,A. and Hsieh,T.S. (1993) DNA topoisomerase I is essential in Drosophila melanogaster. *Proc. Natl. Acad. Sci. U.S.A.*, **90**, 6656–6660.
43. Zhang,H., Meng,L.H. and Pommier,Y. (2007) Mitochondrial topoisomerases and alternative splicing of the human TOP1mt gene. *Biochimie*, **89**, 474–481.
44. Zhang,S., Liu,X., Bawa-Khalfe,T., Lu,L.S., Lyu,Y.L., Liu,L.F. and Yeh,E.T. (2012) Identification of the molecular basis of doxorubicin-induced cardiotoxicity. *Nat. Med.*, **18**, 1639–1642.
45. Miao,Z.H., Player,A., Shankavaram,U., Wang,Y.H., Zimonjic,D.B., Lorenzi,P.L., Liao,Z.Y., Liu,H., Shimura,T., Zhang,H.L. *et al.* (2007) Nonclassic functions of human topoisomerase I: genome-wide and pharmacologic analyses. *Cancer Res.*, **67**, 8752–8761.
46. Castora,F.J., Lazarus,G.M. and Kunes,D. (1985) The presence of two mitochondrial DNA topoisomerases in human acute leukemia cells. *Biochem. Biophys. Res. Commun.*, **130**, 854–866.
47. Lin,J.H. and Castora,F.J. (1991) DNA topoisomerase II from mammalian mitochondria is inhibited by the antitumor drugs, m-AMSA and VM-26. *Biochem. Biophys. Res. Commun.*, **176**, 690–697.
48. Capranico,G., Tinelli,S., Austin,C.A., Fisher,M.L. and Zunino,F. (1992) Different patterns of gene expression of topoisomerase II isoforms in differentiated tissues during murine development. *Biochim. Biophys. Acta*, **1132**, 43–48.
49. Avadhani,N.G., Sangar,M.C., Bansal,S. and Bajpai,P. (2011) Bimodal targeting of cytochrome P450s to endoplasmic reticulum and mitochondria: the concept of chimeric signals. *FEBS J.*, **278**, 4218–4229.
50. Lee,S., Jung,S.R., Heo,K., Byl,J.A., Deweese,J.E., Osheroff,N. and Hohng,S. (2012) DNA cleavage and opening reactions of human topoisomerase IIalpha are regulated via Mg2+-mediated dynamic bending of gate-DNA. *Proc. Natl. Acad. Sci. U.S.A.*, **109**, 2925–2930.
51. Germe,T., Miller,K. and Cooper,J.P. (2009) A non-canonical function of topoisomerase II in disentangling dysfunctional telomeres. *EMBO J.*, **28**, 2803–2811.
52. Ye,J., Lenain,C., Bauwens,S., Rizzo,A., Saint-Leger,A., Poulet,A., Benarroch,D., Magdinier,F., Morere,J., Amiard,S. *et al.* (2010) TRF2 and apollo cooperate with topoisomerase 2alpha to protect human telomeres from replicative damage. *Cell*, **142**, 230–242.